Miner Deposita (2011) 46:639–657
DOI 10.1007/s00126-010-0292-9

ARTICLE

What processes at mid-ocean ridges tell us about volcanogenic massive sulfide deposits

Lawrence M. Cathles

Received: 21 April 2010 / Accepted: 27 May 2010 / Published online: 24 June 2010

Abstract Episodic seafloor spreading, ridge topography, and fault movement at ridges find (more extreme) analogs in the arc and back-arc setting where the volcanogenic massive sulfide (VMS) deposits that we mine today were formed. The factors affecting sulfide accumulation efficiency and the extent to which sulfides are concentrated spatially are the same in both settings, however. The processes occurring at mid-ocean ridges therefore provide a useful insight into those producing VMS deposits in arcs and back-arcs. The critical observation investigated here is that all the heat introduced by seafloor spreading at mid-ocean ridges is carried out of the crust within a few hundred meters of the ridge axis by ~350°C hydrothermal fluids. The high-temperature ridge hydrothermal systems are tied to the presence of magma at the ridge axis and greatly reduce the size and control the shape of axial magma intrusions. The amount of heat introduced to each square kilometer of ocean crust during its formation can be calculated, and its removal by high-temperature convection allows calculation of the total base metal endowment of the ocean basins. Using reasonable metal deposition efficiencies, we conclude that the ocean floor is a giant VMS district with metal resources >600 times the total known VMS reserves on land and a copper resource which would last >6,000 years at current production rates.

Editorial handling: F. Tornos

L. M. Cathles (✉)
Cornell University,
Ithaca, NY 14853, USA
e-mail: lmc19@cornell.edu

Introduction

Volcanogenic massive sulfide (VMS) deposits are a particularly interesting kind of ore deposit because, viewed broadly, they are the direct product of one of the most important global processes. They form in areas of lithosphere extension where partial melts of the mantle produce new crust. Heat introduced by the melts circulates seawater through the crust, and the intimate interaction of the seawater with recently quenched and thermally fractured melt extracts metals. Over the last 50 years, we have learned a great deal about VMS deposits by observing hydrothermal systems in areas of extension at mid-ocean ridges and back-arc spreading centers where the ancient deposits that we have long mined on land are in the process of forming and by comparing this information with the ore deposits and geothermal systems that we are mining or exploiting on land. Many disciplines (geophysics, geochemistry, petrology, heat and mass transfer, numerical methods, economic geology, and biology) and several different communities (geothermal, ore deposit, ocean, modeling) have been involved, and large literatures have developed in which many issues remain in vigorous contention and between which (and between older and recent literature) there is often incomplete exchange. Despite excellent and recent reviews (e.g., Franklin et al. 2005; Hanington et al. 2005), it remains difficult to distinguish the fundamental from the interesting details. The purpose of this paper is to articulate a perspective of what is fundamental from the hydrothermal/ore-formation point of view. In this process, other viewpoints and interesting sidelights will be mentioned to provide entry points into other areas of interest, but this mention will be brief.

The key to the analysis presented is that ~350°C seawater convection can be seen to extract and discharge into the ocean, at the ridge axes, all the magmatic heat introduced into the

crust by seafloor spreading. VMS-type deposits are produced when 350°C seawater discharges into the ocean within a few hundred meters of the axis. The convection through the crust near the ridge is so vigorous that the crust is actually over-cooled and heats up as it moves further from the ridge. This, the inhibited seafloor subsidence it causes, and the small size of axial magma chambers substantiate the crustal-heat-extraction-at-the-axis thesis. The fact that the heat introduced into the crust at the ridge equals that lost by 350°C venting means that the thickness of the crust alone determines the mass of 350°C seawater circulated, on average, through each square meter of seafloor. Combined with the observed chemistry of the high-temperature axial vents, this mass of 350°C seawater places an upper bound on the tons of metal that could be transported to or across each square meter of seafloor. This is an extremely useful number from a resource point of view. For example, it immediately allows us to estimate the ocean metal resources and show that they are almost certainly huge compared to the reserves so far defined on land. From an ore deposit perspective, questions are mainly reduced to: What fraction of the metal carried by the venting fluid is actually accumulated on the seafloor (what is the accumulation efficiency) and to what extent are the accumulated metal sulfides concentrated spatially (how are the sulfides swept into piles)?

The ridge hydrothermal system is remarkably dynamic, and many scientific questions remain open. Whether fluid properties or temperature- and deformation-controlled rock permeability control the ~350°C venting temperature is not clear. The impact of convection parallel to and along the ridge crest compared to the convection perpendicular to the ridge which controls the magma chamber size and crustal heat extraction needs to be assessed, as does the role of brine formation and mineral precipitation in controlling seawater circulation. The episodicity of seafloor spreading and the processes that produce sills must have controlling factors that could be more clearly articulated. The processes at mid-ocean ridges are applicable to the back-arc environment, where some become more extreme in nature. These issues will be discussed and the most important controlling themes sought. The objectives of this paper are, by focusing on the most controlling physical processes, to show where our current understanding is inadequate, to place discovered VMS reserves in a global resource context, and to provide insights that could be useful in exploration.

Convection perpendicular to mid-ocean spreading centers

Even before 1979 when black smokers were discovered on the East Pacific Ridge near 21° N (see brief review by Solomon 1980), it was apparent that a great deal of heat was being carried out of the oceanic crust near ridges by seawater convection. Ocean heat flow had been measured in many locations, and by comparing the measured heat flow data to the heat flow theoretically expected near ridges if the crust were cooling by conduction (Fig. 1), Wolery and Sleep (1976) estimated that hydrothermal convection removes $5.3\pm0.5\times10^{12}$ J s^{-1} from the ocean crust; 5.7×10^{19} J km^{-2} is removed each year from the 2.94 km^2 of new ocean crust produced by seafloor spreading. From their figure (reproduced here as Fig. 1), it is clear that much, but by no means all, of the heat is extracted at the ridge axis.

Heat flow measurements are made in sediment, and few ridges have sediment very close to their axis. An exception is the Galapagos spreading center, and measurements and modeling there show that the heat flow is depressed very near the axis by convection. The data show that the heat flow and the temperature of the crust are actually least near the axis and increase with distance from the axis (Fig. 2). The ridge operates like an early New England fireplace whose main function is to cool the house (crust) by pumping air up the chimney (axial 350°C vents and associated diffuse flow) and drawing cold air into the rest of the house. As indicated in Fig. 2, modeling shows that convection which penetrates the entire crust operates in just this fashion and can explain the observed heat flow pattern very well.

A word on the calculations: As discussed in detail in Fehn et al. (1983), heat is advected across the ridge axis (the vertical left boundary in Fig. 2) at the half spreading rate. Advection includes latent heat. Heat is advected by the motion of the solid crust across the full calculation domain, in addition to being advected by any pore water convection that may also occur through the crust. A heat flow boundary condition at the base of Fig. 2 introduces heat at the rate dictated by the conductive cooling of the sub-Moho lithosphere. Fluid flow is freely allowed into and out of the ocean (top boundary). The left boundary is insulating and impermeable; the top boundary temperature is set at 0°C. The permeability of the ocean crust decreases exponentially with depth from 5×10^{-15} m^2, as shown in the figure. The model is run until quasi-steady state is reached in which the average temperature and average total mass flux are constant. The plate motion causes the convective pattern to continually shift position relative to the axis of spreading, but this is unimportant to the present discussion because it produces minor perturbations in a thoroughly cooled crust. The amplitude and wavelength of the off-axis circulation indicates that the average off-axis crustal permeability is ~0.17×10^{-15} (0.17 mD) and that convection occurs to ~3.5 km depth (Ribando et al. 1976; see also Cathles 1981).

The model shown in Fig. 2 is designed to investigate how seawater convection (in a vertical plane perpendicular to the ridge axis) controls the temperature of the ocean crust

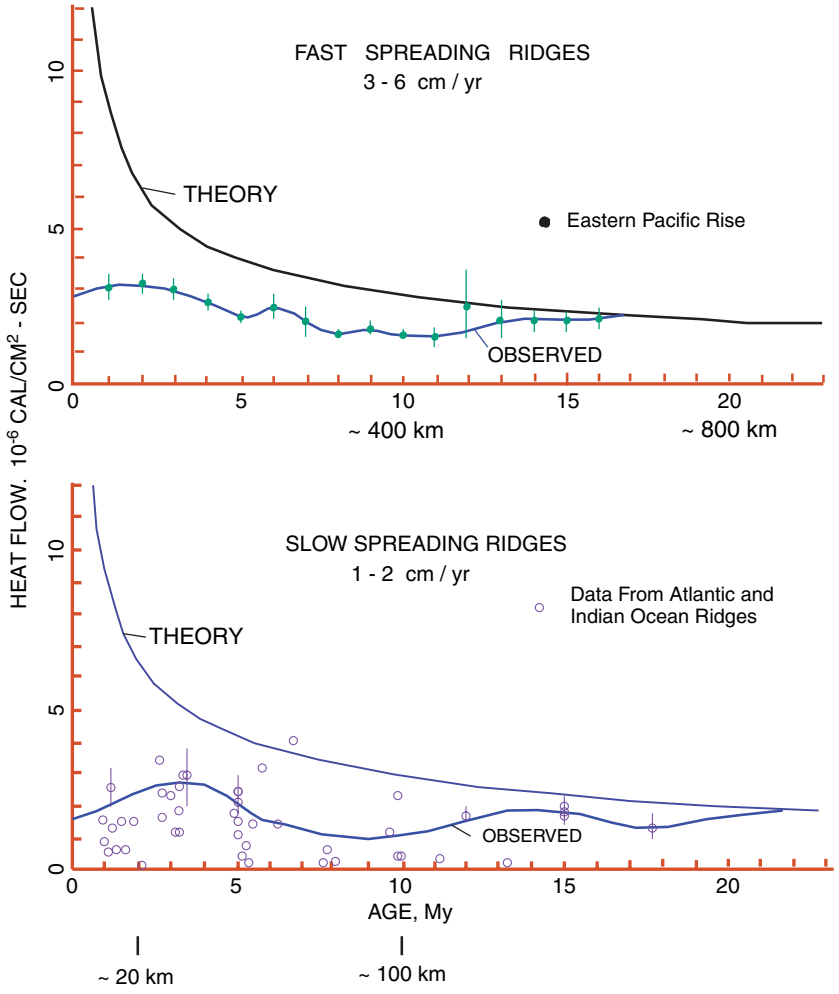

Fig. 1 Heat flow measured on the seafloor as a function of its age compared to that expected from a conductively cooling plate (theory). The gap between observation and theory, integrated over all oceans, was estimated by Wolery and Sleep (1976) at 5.3×10^{12} W. Figure modified from Wolery and Sleep (1976)

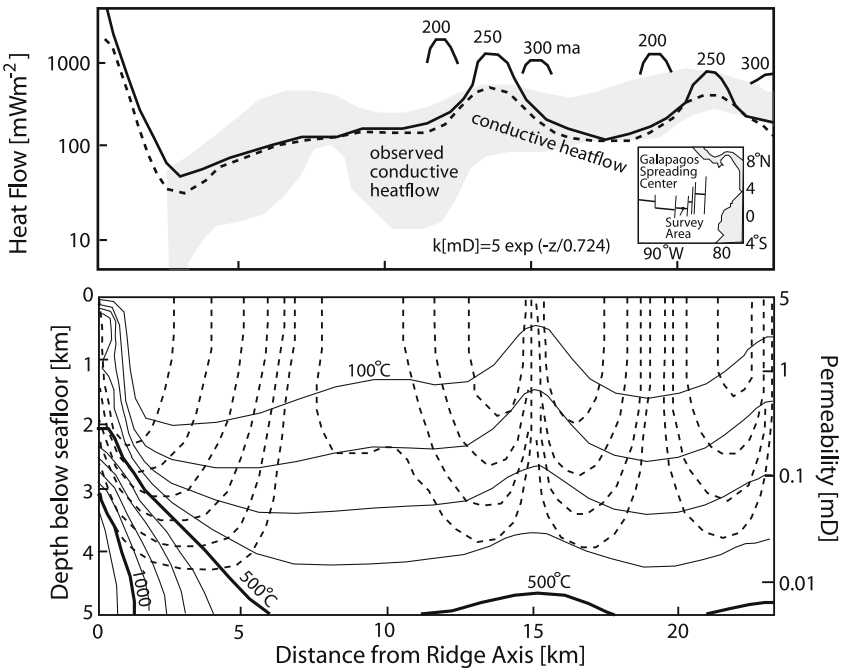

Fig. 2 Heat flow in a 20-km^2 area near the Galapagos spreading center, projected to a transect perpendicular to the ridge (*top panel*) shows that heat flow is dramatically depressed near the ridge axis and is lowest very near the axis. Models of convection through the entire crust (*lower panel*) replicate the observed pattern (*curves in top panel*). The *dashed lines* are streamlines that indicate the pattern of flow. The *numbers at peaks of the solid heat flow curve* mark their positions at 200, 250, and 300 Ma after the start of the simulation. The crustal permeability decreases exponentially from 5 mD at the seafloor to 5×10^{-3} mD at 5 km depth as indicated by the formula. Figure is from Fehn et al. (1983)

near a mid-ocean ridge. The important physics is contained in the left (ridge) boundary condition. This boundary condition assumes that magma from the mantle is injected laterally at the spreading rate. Of course in reality the magma must also move upward through a zone of some thickness adjacent to the boundary. In the sheeted dike layer (where the calculated crustal temperature is <400°C), this zone is very thin and has the width of a sheeted dike. In the underlying gabbro layer, it can be much broader, and here, the upward motion envisioned is that of a magma filtering through the pores of a cumulate intrusion.

In addition to showing that convection in the crust matches the observed heat flow pattern, Fig. 2 also shows that near-ridge convection dramatically reduces the size and changes the shape of the axial magma intrusion. By magma intrusion, we mean the zone within which magma is present either in a chamber or melt lens or in the pores of a cumulate intrusion. On our diagrams, its shape is proxied by an isotherm. The bold 500°C isotherm serves this function in Fig. 2. Figure 3 illustrates how crustal permeability controls the shape of the axial intrusion. The

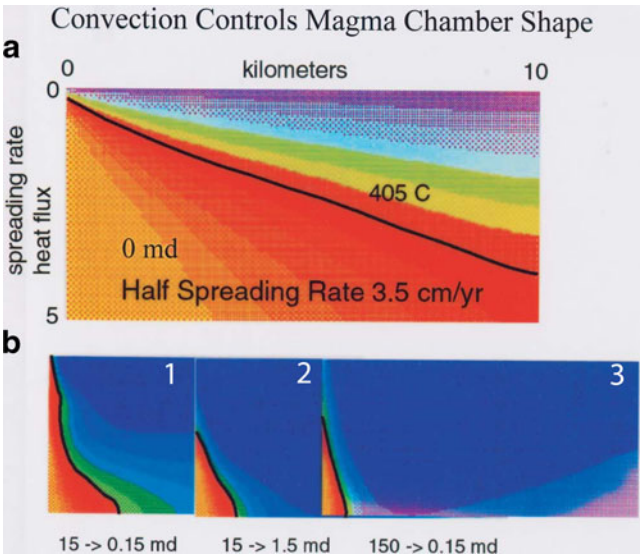

Fig. 3 Finite difference model showing the effects of convection on the shape of the axial magma chamber at a mid-ocean ridge. In this model, heat is advected laterally across the left boundary at a rate equivalent to 1,200°C magma moving across the boundary at 3.5 cm/year. Heat is advected across the diagram at the rate of seafloor spreading as well as by seawater convection through the crust. The temperature pattern shown is the steady-state pattern. The boundary between the sheeted dike and gabbro layers is marked by where the black 405°C isotherm intersects the axis. Above this contour, the plate cools quickly at the axis and magma is emplaced as basaltic dikes. Below this contour, the crust cools slowly and the gabbro layer is formed. **a** The *top panel* shows the temperature pattern for an impermeable crust. The *lower panel* (**b***1*, *2*, *3*) shows the pattern for crustal permeabilities decreasing exponentially from the top to the bottom of the crust by the amounts indicated. The methods of calculation are described in Cathles (1983)

methods are the same as those in Fig. 2 and are unpublished calculations performed by the author at about the same time as those in Fig. 2.

Figure 3 shows that if the crust were impermeable enough that no thermally significant convection occurred, the magma intrusion (proxied by the 405°C isotherm in this figure) would be very broad and have a thin overlying sheeted dike layer. Heat flow would decrease linearly with distance from the very high ("theoretical") values in Fig. 2. This pattern would be very different from that observed at the Galapagos spreading center shown in Fig. 2a. If the crust were only slightly permeable, the axis would be sufficiently thermally shielded by the weak convection for the sheeted dike layer to be reduced in thickness or even eliminated (Fig. 3b1). The crust would consist of only a gabbro layer capped by pillow basalts. If the crust were very permeable (not shown), the gabbro layer would be eliminated entirely, and the crust would consist of sheeted dikes capped by extrusive flows. If the typical oceanic crust consists of 0.7 km of extrusive flows, 1.2 km of dikes, and 4.6 km of gabbros as generalized by Mottl (2003), the crustal permeability must be the heat transport equivalent to that shown in the second and third lower panels, Fig. 3b2, b3. There is clearly a very strong connection between magma intrusion shape, hydrothermal convection perpendicular to the ridge axis, crustal permeability, and spreading rate.

The cooling of the entire crust at or very near the ridge axis is reflected directly in the heat flow pattern from 2 to 30 km (0.7 to 1 Ma) in the Galapagos area of the East Pacific Rise (Fig. 2), but is this rapid cooling of the crust very near the ridge axis typical? A similar pattern has been noted by Davis et al. (1999) of the Juan de Fuca Ridge but differently interpreted as we will discuss. Cochran and Buck (2001) marshal seafloor subsidence rate data from intermediate-, fast-, and extremely fast-spreading segments of the Southeast Indian Ridge and the East Pacific Rise (including 12°40′ to 15°10′ N) to suggest that the rapid cooling is indeed a general phenomenon. Their analysis is a clever one. At crustal ages >~1.4 Ma, the depth to the seafloor (corrected isostatically for sediment and water loading) decays as the inverse square root of time, exactly as expected for conductive cooling and thermal contraction. Seafloor elevation plots linearly with the square root of time. Worldwide the average slope is 350 m $Ma^{-0.5}$, but the mean subsidence rate of seafloor younger than 1 to 1.4 Ma is <220 m $Ma^{-0.5}$. Cochran and Buck suggest that the reason for this reduced subsidence rate is that the crust is completely cooled within 5 km of the ridge axis and is reheating over the next million years, just as in the Galapagos area. Immediately adjacent to the ridge axis, the reshuffling of heat from the lithosphere to the reheating crust reduces the subsidence rate. Cochran and Buck use a

1D thermal conductivity model with a Nusselt number of 15 to 30 applied for 0.1 Ma to simulate the near-ridge convective cooling of the crust and show that the subsidence rate is reduced in the very young (0.1 to ~1 Ma) crust just as is observed. The significance of Cochran and Buck's analysis is that it suggests that the crust at intermediate-, fast-, and very fast-spreading ridges is cooled at the ridge axis just as it does at the Galapagos.

Seismic tomography (Fig. 4) shows that the melt fraction in the gabbro layer (layer 3) on the East Pacific Rise at 9°30′ N is greater than zero only 2.5 to 3 km from the ridge axis, although in the mantle it extends ~9 km from the ridge (Dunn et al. 2000). A narrow crustal melt zone and a much broader melt zone in the underlying mantle is also evident at 17° S (Dunn and Forsyth 2003). This is exactly the situation one would expect if the crust was rapidly cooled by seawater convection within a few kilometers of the ridge axis.

Another very strong piece of evidence that convection cools the crust very near the axes of mid-ocean ridges is the observation that high-temperature vents invariably lie within a few hundred meters of the spreading axis. Surprisingly, this seems to be more the case for faster spreading rates. One of the very few significantly off-axis high-temperature vents that have been discovered is the TAG black smoker mound which lies ~2.4 km east of the rift valley of the slow-spreading (10–20 mm year^{-1} half rate) Mid-Atlantic Ridge at 26°08′ N. At 21°N on the East Pacific Rise, where the (half) spreading rate is 30 mm year^{-1}, the high-temperature vents are located right on the primary fissures of the current rift axis that feeds young sheet and lobate lava flows. This axis is slightly displaced from the center of a 100-m-deep, 3-km-wide summit graben that sits on the top of a ~5-km-wide ridge-crest dome. At fast-spreading sites, vents are often in narrow axial clefts which are thought to be collapse features produced when lavas erupted at the axis drain back into their source. For example at 17.5°S on the East Pacific Rise

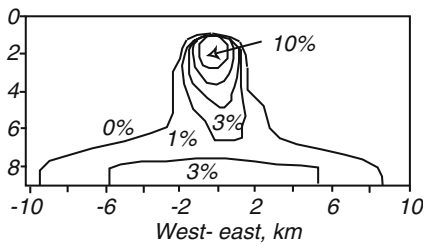

Fig. 4 Seismic tomographic interpretation of the fraction melt below the ridge crest at ~9°30′ N on the East Pacific Rise assuming the melt is present as films around cumulate grains and that anelasticity is important, assumptions which minimize the melt fraction but do not affect the melt geometry. Note that the magma intrusion is narrow (<2.5 km) in the crust and broadens to nearly 10 km in the mantle. Figure from Dunn et al. (2000)

(>75 mm year^{-1} half spreading rate), nearly pervasive high-temperature hydrothermal venting is occurring along a very narrow (<50–100 m wide) cleft 7–12 m deep right on the spreading axis. There are no large sulfide chimneys, which suggest that this venting is very recent. Fornari and Embley (1995) provide an excellent review of hydrothermal processes observed at mid-ocean ridges, from which the above summary was taken. They emphasize that hydrothermal venting more than a few hundred meters of the spreading axis has been observed in only a very few locations. The high-temperature hydrothermal venting is on the white line in the middle of a thin highway on the axis of seafloor spreading.

The axial nature of the high-temperature hydrothermal venting is important to our current discussion because it means that the top of the axial magma chamber cannot be very broad. Modeling shows that the strong convection at the edge of tabular intrusions that are as wide as or wider than the depth of their top below the seafloor produces discharge above the edges of the intrusion. Seawater is drawn into the crust at the axis (e.g., Cathles 1978) and is discharged above the edge of the intrusion kilometers from the axis. Priming of the subsequently permeable axial fractures with magma may reduce this tendency somewhat, but nevertheless, the observation that the hydrothermal discharge is within at most a few hundred meters of the axis of seafloor spreading is very strong evidence that the axial magma intrusion below the ridge axis is narrow (although it might broaden at greater depths as shown in Fig. 2). The fact that a substantial fraction of the axial discharge originates from flow deep in the crust along the edge of the magma intrusion that produces the gabbro layer suggests that the ridge axis is not a good place to sequester brines or maintain a two layered (brine and seawater) convection system. The seawater circulation perpendicular to the ridge axis is single pass. The seawater moves into the crust from distances of up to 5 km from the axis, heats within a kilometer or so of the ridge axis, and discharges at or very near (within ~100 m of) the ridge axis. As discussed later, buoyant forces in the 350°C flow zone that forms at the edge of the axial intrusion are large enough to clear any flow impediments within ~600 m of the seafloor. A deep (to the Moho) convective system is able to "clear its throat", and this may account for minor "explosive" breccias seen in VMS vent sites such as Buttercup Hill in Noranda (Gibson et al. 1989).

Convection parallel to mid-ocean spreading centers and other conceptions of processes at the ridge axis

Many models have been constructed of the near-mid-ocean ridge crust. Cherkaui et al. (2003) present a ridge-

perpendicular convection model very similar to the one discussed above, for example. But other current models are quite different. Before deriving the logical implications of the ridge-perpendicular convection just described, it is important to discuss these alternative concepts.

In fact most of the mid-ocean ridge oceanographic community appears to currently have a very different view to that articulated above. Almost all the recent (last 10 years or so) papers have addressed ridge-parallel convection in which seawater circulates into the ridge axis, descends to and moves along the top of a melt lens in a thin "high-temperature reaction zone", perhaps cooling and cracking into the lens with time, and then moves to the surface to feed a black smoker vent or cluster of vents on the ridge axis (e.g., Lowell and Burnell 1991; Lowell and Germanovich 1994). Particular interest has focused on how the temperature of venting is controlled and particularly on whether phase separation, brine formation, and/or realistic fluid properties could achieve the necessary control. For example, Wilcock (1998) showed that with realistic fluid properties the venting temperature can be expected to be 0.5 to 0.65 times the temperature of the basal (melt lens) boundary. To account for the maximum venting temperatures observed (320–380°C), they conclude that the boundary must have a temperature of between 490°C and 760°C. Fontaine et al. (2007) argued that the permeable sheeted dike layer was needed to reduce brine salinity to the observed range of 0.1 to 8 wt.% NaCl, but then a sheath of anhydrite is needed to maintain venting temperatures. They conclude that "very specific permeability configurations are required to match both the temperature and maximum salinity" of venting. Fontaine and Wilcock (2007) discuss the dilemma further. They attribute the ~700°C basal temperature to the brittle–ductile transition that occurs in this temperature range (Hirth et al. 1998).

Fontaine and Wilcock (2006) addressed whether a brine layer could assist in controlling the temperature of venting but found through ridge-parallel two-phase modeling that the brine layer would be stagnant and would accumulate rapidly and quickly throttle the venting temperature too much. The brine needs to be drained laterally or axially. Since in at least one case (Von Damm et al. 1997) low-salinity (condensed vapor) venting was replaced 3 years later by brine venting at the same site, Fontaine and Wilcock suggested that the brine might be temporarily sequestered in smaller aperture fractures and pores and flushed out by convection driven by an adjacent cold water head when the venting of vapor is finished. They note that a cold water head can expel hot brines up to 30 wt% salinity.

On the other hand, very careful two-phase pure water modeling by Cormou suggests that fluid properties alone can control venting temperatures in the observed range, substantiating a proposal made long ago by Bishoff and Rosenbauer (1985) and reiterated recently by Jupp and Schultz (2000). Cormou et al. (2006) model convection driven by a horizontal 1,000°C base 1 to 2 km below the seafloor utilizing pure water fluid properties and a high-resolution mesh. They find the same venting temperatures for rock permeability of 100 (374±20°C), 10 (377±20°C), and 1 (387°C) mD (10^{-15} m^2) and the base either 1 km (377±20°C at 10 mD) or 2 km (375±20°C at 10 mD) below the seafloor. The convection is much more unstable than suggested by lower-resolution modeling, and the upwelling zone can split and stop as they rise and extinguish and then restart (see also Fontaine and Wilcock 2007). With realistic fluid properties, the plumes are more closely spaced (Cormou et al. 2008a). The secret of the temperature control is a sheath of warm downwelling seawater surrounding the upwelling plumes, a feature most dramatically seen in 3D simulations (Cormou et al. 2008b). The temperature of venting appears to adjust so that the heat transport is maximized (e.g., the Nusselt number is maximum). Cormou's 3D simulations are carried out in a box 4 km long (along the ridge), 3 km wide (perpendicular to the ridge), and 1 km deep (below the seafloor). The ridge is simulated by imposing 1-km-wide Gaussian heat flux along the ridge axis running through the bottom center of the computational box.

The top of the melt lens need not be at the same depth everywhere along the ridge axis. If its top is sloped, the number of plumes is reduced, ultimately to just one centered over its shallowest point (Fontaine et al. 2009). Subsurface mineral redistribution by hydrothermal circulation will be small (Cathles 1983), but mineral precipitation as hot plumes move toward the surface can still be substantial enough to impair permeability if flow is restricted to fractures (as it is in igneous rocks, Fontaine et al. 2001). Flow-through fractures with low porosity also completely change the dynamics of thermohaline convection because it allows solutes to be advected much faster than heat (Schoofs et al. 1999). The result is that if the system is capable of producing salinity differences of >4 wt.% and the fracture porosity is <1%, convection is chaotic with fronts of salinity sweeping across the system and the temperature of venting changing in an oscillatory and chaotic fashion. These conditions may not pertain to the ocean ridge environment, but they could explain the very curious changes in chemistry noted in caldera veins in Creed Colorado. In addition, experiments show that, once created, brine is sequestered in lower-permeability stagnant areas and has its own dynamics that may be hard to capture with models (Emmanuel and Berkowitz 2007).

From all of this, as well as the obvious opportunities for mixing, clogging, and tectonism at an active ridge axis, it is clear that the axial convection is complex and very dynamic. To the focus taken here, however, these matters

are details that are not significant. The ridge-perpendicular convection will supply much if not most of the heat discharged at high temperature along the ridge axis because the thickness of the gabbro layer cooled by this convection is much larger than the thickness of the overlying sheeted dike layer. Some heat may be mined from the gabbro layer by axial convection, but, by heat balance, most must come from the crust underlying the melt lens. The dynamics just reviewed is vital to the proper interpretation of crustal alteration and for locating the discharge points that will host major deposits. But the complex dynamics will not change the amount of heat discharged at high temperature at the ridge axes.

An alternative explanation for the heat flow deficit shown in Fig. 1, however, would be a serious challenge to the basis thesis of this paper, and such an alternative explanation has been offered by Davis et al. (1999) and Rosenberg et al. (2000). They suggest that the depression of heat flow relative to the conductive cooling curve of the lithosphere is not due to the convective cooling of the entire crust as we suggest but rather due to the flow of cold seawater that enters unsedimented zones near the ridge axis and moves away from the ridge through permeable layers in the crust under sediment-covered zones adjacent to it. The drive for this convection is a thermal siphon: The cold zones near the ridge axis have a greater head than the hotter pore fluids under the sediments away from the ridge. Their modeling shows that this convection could depress heat flow in the fashion observed if a 500-m-thick portion of the sheeted dike/pillow basalt layer had a permeability of between 10 mD and 1 darcy. They do not discuss (and it is not clear) how their thermosyphon would be initiated. They find their explanation more plausible than convective cooling of the entire crust. If their suggestion is correct, separate explanations must be offered for the small size of the axial magma chamber and the subsidence pattern away from the ridge, and I find their suggestion, although possible, unconvincing.

Different views have been presented for the flow of melt at the ridge axis. These views fall into the category of interesting details in the context of this paper, but they are important for interpreting field observations in ophiolites and might impact detailed models of ridge convection. One is the so-called glacier model which injects all latent heat into a small 500-m-wide, 150-m-thick melt lens and thin (sheeted) dikes above this lens (e.g., Chen 2000; Phipps Morgan and Chen 1993). The magma lens lies at the top of the gabbro layer and is 100% melt (0% cumulate). Latent heat is released before the melt leaves the lens or overlying dikes. This concept was investigated by calculating the temperature distribution it would produce using a 1D vertical conductive heat flow model in which seawater convection is captured by enhancing the thermal conductivity in regions where there is thought to be aqueous fluid flow. In non-dimensional form, this translates to increasing the Nusselt number (the ratio of advective to conductive heat flow) in the regions where convection is assumed to be taking place. Ductile flow is computed where the crust is hotter than 600°C using a power law rheology with a strong temperature dependence. This leads to a greatly augmented lateral flow through the melt lens and to the conclusion that the underlying cumulate gabbro (our magma intrusion) grows, like a glacier; it grows from the downward movement of cumulate crystals produced in the melt lens.

The 400°C isotherm produced by these models is similar to that in the upper conductive panel in Fig. 3. Hence, the heat flow pattern near the ridge would not be compatible with the Galapagos data. The glacier model does simulate the observed dependence of the depth to the melt lens on spreading rate, including the abrupt disappearance of the melt lens at lower spreading rates which is related to non-linearities in the viscosity–latent heat release relationship. The axial graben disappears at almost exactly the same spreading rate at which the melt lens appears (compare Small 1998 to Chen 2000), however. Movement on the boundary faults of the axial graben probably increases the permeability of the crust near the ridge, and the enhanced seawater convection this allows might also extinguish the melt lens. Thus, other non-linearities could also account for the observed relationships.

Recent petrologic work suggests that melt movements may not be those envisioned in the glacier model. Pan and Batiza (2003) unexpectedly found no difference in the complexity of crystal composition between lavas at axial sites that have a shallow melt lens and those that do not. The compositional complexity is thought to result when melt passes through the cumulate. If the glacier model is correct, the crystal composition should not be as complex when there is no melt lens, but this was not found to be the case. Pan and Batiza conclude that the melt lens results from compaction of the cumulate crystals in the magma chamber and that melt passes upward through the cumulate from the mantle into the overlying sheeted dikes and surface extrusives. The melt passes through the cumulate whether or not the cumulate (gabbro layer or layer 3) is capped by a melt lens. Thus, there is no difference in petrologic complexity whether a melt lens is present or not. They argue in a separate paper that a xenolith found in a relatively primitive and unusually gassy normal mid-ocean ridge basalt sheet flow that erupted in 1991 at 9°50′ N on the East Pacific Rise supports this picture. The xenolith shows two stages of plagioclase growth followed by re-melting and contains cumulate anorthite. It suggests that repeated pulses of Ca-rich melts from depleted mantle beneath the ridge have passed upward through the cumulate (Ridley et al. 2006).

The two views of melt and cumulate movement could lead to different depth profiles of heat removal from the gabbro layer. More heat might be removed from the melt lens in the glacier model, for example, because latent heat release would be more focused there. But redistributing the pattern of heat release within the gabbro layer does not alter the total heat released, which is the important point here.

Quantitative aspects of crustal cooling at ridge axes

The $5.3\pm0.5\times10^{12}$-W rate that Wolery and Sleep (1976) estimated heat is carried out of the ocean crust by high- and low-temperature hydrothermal convection (the heat flow deficit in Fig. 1) has been revised upward to 11×10^{12} W, based on more data, a greater sealing age (age at which heat flow joins the conductive curve) in some oceans, and a hotter mantle (1,450°C vs 1,200°C; Stein and Stein 1994). Stein and Stein estimate the rate at which heat carried out of the crust at the ridge axis through crust <1 Ma old is $3.2\pm0.3\times10^{12}$ W (about 30% of the total 11×10^{12} W). As noted by many, the convective fluid venting at lower temperatures away from the ridge axis is much more voluminous than that at the ridge axis. More than three times more heat is removed, and the temperature of venting is much lower.

Table 1 analyzes the mid-ocean axial convection system quantitatively. The first parts of the Table 1 follow Mottl (2003) and Elderfield and Schultz (1996) quite closely, and additional very good discussion is available in these references. The first ten rows of Table 1 provide a quantitative analysis of the rate at which heat is introduced into the crust by seafloor spreading. The parameters needed to compute the rate are first given. Note extrusive flows are not counted (row 8). It is assumed that they are quenched by seawater as they are erupted and that their heat therefore does not drive organized convection and focused venting. Latent heat of crystallization and mineral alteration is included (row 3). The result (row 10) is that the rate at which heat is introduced into the crust by seafloor spreading, Q_T, is 2.4 to 3.1×10^{12} W, which is nearly identical to the $3.2\pm0.3\times10^{12}$ W that Stein and Stein (1994) estimated is carried out of crust <1 Ma old by high-temperature vent fluids (row 11). The hypothesis that the crust is completely cooled by convection at the ridge axis and that this heat is vented at ~350°C is strongly supported by this identity.

The rows in Table 1 below row 11 analyze the implications of crustal heat extraction for ore deposition. By dividing the heat introduced by seafloor spreading by the heat necessary to warm seawater to 350°C, row 13 shows that the mass of 350°C fluids vented per square meter of ocean plate is $>1.5\times10^{7}$ kg m^{-2} (>15 mt/m^2, greater because we have used the lower end of the range of Q_T). This is about 1 kg of 350°C vent fluid per kilogram of non-extrusive crust, a result which can be obtained either by noting that the non-extrusive thickness of the crust (H') times the density of the crust (ρ_r) equals 1.62×10^{7} kg m^{-2} which is $\sim1.5\times10^{7}$ kg m^{-2}, or by dividing the heat introduced to each kilogram of crust, 1,000 h_T, by the heat required to heat 1 kg of seawater to 350°C, h_{sw}. This simple and very useful relationship that 1 kg of 350°C discharge requires 1 kg of magma intrusion was first pointed out by John Elder (1966) in his pioneering analysis of the Wairakei geothermal system. This relationship might be called Elder's Rule, as is done in Table 1.

The known chemistry of the 350°C vent fluids are given in the 14th row of the table. Rows 16–20 compute the surface densities of these elements and the minerals they form. These rows show that venting 1.5×10^{7} kg m^{-2} of 350°C fluids with the chemistry bracketed in row 14 will precipitate near to or carry across the seafloor 1,344 to 11,640 kg m^{-2} of pyrite and up to 105 kg of zinc and 42 kg of copper per square meter of ocean crust (see metal surface density entries σ_{Fe}, σ_{Zn}, and σ_{Cu} in Table 1).

Massive sulfide districts have ore surface densities an order of magnitude or two lower than this. This is shown in row 21 which gives estimates of pyrite and metal surface densities in typical VMS mining districts (e.g., ~110 kg-FeS_2 m^{-2} and metal surface densities of ~2 kg Cu and 2.5 kg Zn m^{-2} of the mining district; Sangster 1980). Thus, if well-explored VMS districts are a good guide, the potential of the mid-ocean ridge spreading centers to make VMS deposits is enormous compared to the fraction of that potential which is typically realized. This can be seen clearly when the metal surface densities are plotted. As shown in Fig. 5, the Cu, Zn, and Fe transported to or across each square meter of the seafloor by 350°C fluids at the ridge axis is one to two orders of magnitude greater than that in VMS districts. This is not surprising because it has long been realized that relatively little of the metal content in black smoker fluids is accumulated as sulfides on the seafloor near the vents. For example, Converse et al. (1984) estimated that about 3% of the base metals accumulate in sulfides near the vents at 21° N.

If even 3% of the metals vented at ridges accumulate as sulfides, however, the resource potential of the ocean crust would be enormous compared to what we have so far discovered on land. For example, Franklin et al. (2005) indicate that VMS deposits of all types contain discovered reserves of $\sim850\times10^{6}$ t metal. Taking the low end of the black smoker metal flux to the seafloor (39.2 kg m^{-2} Zn and 9.8 kg m^{-2} Cu), assuming 3% of this metal accumulates on the seafloor, and multiplying by the 3.6×10^{8} km^2 area of the ocean crust (all of which was produced by seafloor spreading) yield a total metal tonnage of 530×10^{9} t. This is a potential resource over 600 times greater

Table 1 Calculation of mass of 350°C fluid vented per square kilometer of new ocean crust and metals transported to or across the seafloor by this flux (after Mottl (2003) and Elderfield and Schultz (1996)) and comparison to VMS metal distribution

1. H = thickness of oceanic crust	6.5±0.75 km (0.7 flows, 1.2 dikes, 4.6 gabbro)	Mottl (2003)
2. C_c = heat capacity of mafic crust	1.2±0.15 J g^{-1} K^{-1}	Mottl (2003)
3. L = latent heat crystallization and alteration	420 J g^{-1}	Norton and Cathles (1979)
4. T_o = temperature of ridge magma	1,200°C to 1,450°C	Mottl (2003) to Stein and Stein (1994)
5. h_c = heat released in cooling from T_o to 350°C	1,020 to 1,320 J g^{-1} K^{-1}	= C_c (T_o−350)
6. h_T = total heat released	1,420 to 1,870 J g^{-1} K^{-1}	= $L + h_c$
7. ρ_r = density of ocean crust	2,800 kg m^{-3}	
8. q_T = heat introduced by sea floor spreading to each m^2 of new crust, discounting heat in flows	2.3 to 3.0×10^{13} J m^{-2}	= (H'=5.8×10^3) (2,800) (1,420 to 1,870×10^3) (note: 5.8×10^3=H'=thickness gabbro plus dikes)
9. $\dot{A}$ = area of new ocean crust formed each year including back-arc basins	3.3×10^6 m^2 $year^{-1}$	Parsons (1981)
10. Q_T = rate heat is introduced to the crust by seafloor spreading in watts (joules per second)	2.4 to 3.1×10^{12} W	= $q_T\dot{A}$
11. Q_{350} = rate heat is removed from by ~350°C hydrothermal discharge at the ridge axes	3.2±0.3×10^{12} W	Stein and Stein (1994)
12. h_{sw} = heat required to heat seawater to 350°C beneath ocean ridges	1540±200×10^3 J kg^{-1}	Mottl (2003)
13. m_{350} = mass of 350°C seawater discharged in cooling each m^2 of new ocean crust	>1.5×10^7 kg m^{-2}	= $\frac{q_T}{h_{sw}} \sim H'\rho_r$ (Elder's rule)
14. 350°C vent fluid composition (low and high range) in 10^{-6} mol kg^{-1}	S 2,900, Fe 750, Zn 40, Cu 9.7 low S 12,200, Fe 6,470, Zn 106, Cu 44 hi	Elderfield and Schultz (1996)
15. Percent base metals vented (low and high)	S 93.8%, Fe 5%, Zn 1.21% (19% Cu) S 98.8%, Fe 0.85%, Zn 0.36% (29% Cu)	Elderfield and Schultz (1996) (pyrite, sphalerite, chalcopyrite, % Cu)
16. σ_{Fe} = moles iron vented[a] from each km^2 ocean crust	1.12 to 9.7×10^4 mol m^{-2}	= m_{350} (750 to 6,470×10^{-6} mol kg^{-1})
17. σ_S = moles S vented[a] from each m^2 ocean crust	4.35 to 18.3×10^4 mol m^{-2}	= m_{350} (2,900 to 12,200×10^{-6} mol kg^{-1})
18. σ_{Zn} = moles Zn vented[a] from each m^2 ocean crust	600 to 1,590 mol m^{-2} (39.2 to 104.6 kg m^{-2})	= m_{350} (40 to 106×10^{-6} mol kg^{-1})
19. σ_{Cu} = moles Cu vented[a] from each m^2 ocean crust	145 to 660 mol m^{-2} (9.8 to 41.9 kg m^{-2})	= m_{350} (9.7 to 44×10^{-6} mol kg^{-1})
20. σ_{pyrite} = kg of FeS_2 vented from each m^2 ocean crust	1,344 to 11,640 kg m^{-2}	σ_{Fe} (mol wt pyrite=0.12 kg mol^{-1})
21. σ_{ore} = kg of sulfide in VMS district	110 kg m^{-2} pyrite up to 2 kg m^{-2} Cu up to 2.5 kg m^{-2} Zn	Sangster (1980) Using percent Cu, Zn in ore hosted by bimodal mafic and mafic hosts given in Franklin et al. (2005)
22. Percent base metals		Calculated from Table 2 in Franklin et al. (2005)
Bimodal mafic hosted	Fe 92.6%, Zn 4.84%, Cu 2.58% (29% Cu)	
Mafic hosted	Fe 94.4%, Zn 1.77%, Cu 3.83% (68% Cu)	

[a] Metal and sulfur concentration in black smoker vent fluids from Elderfield and Schultz

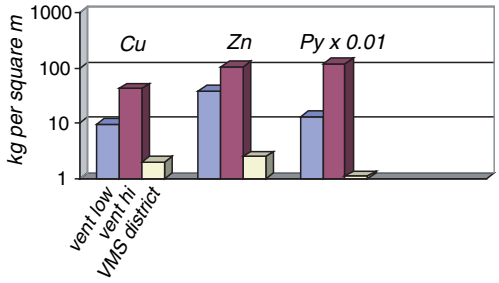

Fig. 5 Comparison of metal flux to the seafloor by 350°C black smoker hydrothermal vents to the average discovered metal surface density in well-explored VMS districts (from Sangster 1980). The ocean metal flux is 1 to 2 orders of magnitude greater, reflecting the low (~3%) efficiency with which base metals typically accumulate as sulfides near the hydrothermal vents

than our current reserves of VMS base metal. Assuming the copper to copper plus zinc ratio is 0.2 (the ratio in the black smoker flux given just above), the ocean crust should contain 106,000 Mt of Cu metal. At the current consumption rate (2009) of ~16 Mt Cu/a, the ocean resource would last more than 6,000 years, while the land-based resource of 3 Gt Cu would last about 200 years.

Finally, the last row in Table 1 gives the percentages of base metals found in VMS districts. The sulfides accumulated in these known VMS districts are enriched in Cu and perhaps Zn, compared to the 350°C vent fluids. Figure 6 plots the data from rows 15 and 22 of Table 1 and shows a clear enrichment of Cu in VMS deposits relative to that expected from ocean vent chemistry. The enrichment of Cu suggests that Cu is trapped in VMS deposits more efficiently than Zn and Fe. As will be discussed briefly again below, this results from the replacement of pyrite and sphalerite by chalcopyrite in the sulfide piles and feeder stockworks as hot vent fluids continue to pass through them. It is the consequence of Barton's dreaded chalcopyrite disease, in which chalcopyrite can be seen to invade pyrite and sphalerite like a cancer, putting iron and zinc into solution and discharging them into the ocean (see Eldridge et al. 1983).

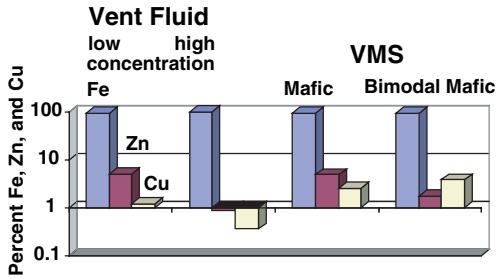

Fig. 6 Proportions of Fe, Zn, and Cu in high-temperature 350°C vent fluids compared to the metal ratios in VMS deposits summarized in Table 1. Copper is enriched in VMS deposits by subsurface replacement of Zn and Fe in subsurface sulfides

Dynamics of the deep mid-ocean ridge hydrothermal system

The dynamics of the mid-ocean ridge-parallel convection system that overlies the melt lens at the top of the axial magma chamber has already been discussed. This section addresses dynamic aspects of the ridge-perpendicular convection that lies below the melt lens. Many of the issues that have been addressed in the lower zone are similar to those that have been discussed in the upper, but some are new. There are some simple principles that have been extracted from studies of geothermal systems over the years that are very useful. A particularly powerful one was deduced by Elder (1966) from observations of the Wairakei geothermal system. He concluded that the width of upwelling hydrothermal plumes is self-adjusting. The idea is that upwelling pore waters will entrain adjacent pore waters unless the vertical pressure gradient in the upflow zone is the same as in adjacent areas, and the width of the upwelling zone will adjust so that this is the case. Figure 7 gives a simple example of this self-focusing. Numerical simulations reflect this behavior (Cathles 1977), and Elder's observation provides an easy way to estimate the rate of vertical flow (Cathles 1981, Appendix). For example, for a 10^{-15} m^2 (1 mD) permeability, the vertical mass flux in a 350°C plume that balances the pressure gradient in the cool adjacent pore fluids will be 640 kg m^{-2} $year^{-1}$. The mass flux would be twice this if the permeability were two times larger, etc. For a fluid density of 800 kg m^{-3}, the volume flux of a hydrothermal fluid is 0.8 m $year^{-1}$. Since water-saturated rock has about half the heat capacity of water, the rise rate of a hydrothermal plume (e.g., the migration rate of the thermal front at the top of the plume) will be about twice the volume flux (Cathles 1997) or 1.6 m $year^{-1}$. Thus, black smoker venting can be expected to start at a dormant ridge ~1,000 years after an episode of seafloor spreading if the top of the gabbro layer is 1.6 km below the seafloor and the permeability is 10^{-15} m^2 (1 mD). At 10^{-14} m^2 permeability, 350°C discharge would be established in ~100 years, and at 10^{-13} m^2, it could be established in ~10 years, etc. The important point is that in areas where seafloor spreading is episodic, high-temperature hydrothermal discharge is likely to be established at the ridge axis long after the pulse of spreading has been completed. This is seen in geothermal systems on land. There is no surface expression of hydrothermal activity above the Salton Sea geothermal system that is being exploited for geothermal energy, for example. No hot springs, geysers, and the like are to be found, only a few recent volcanic flows. The reason may be that magma intrusion at depth is very recent, and the geothermal system has not had time to migrate to the surface. See Cathles (1977) for more discussion.

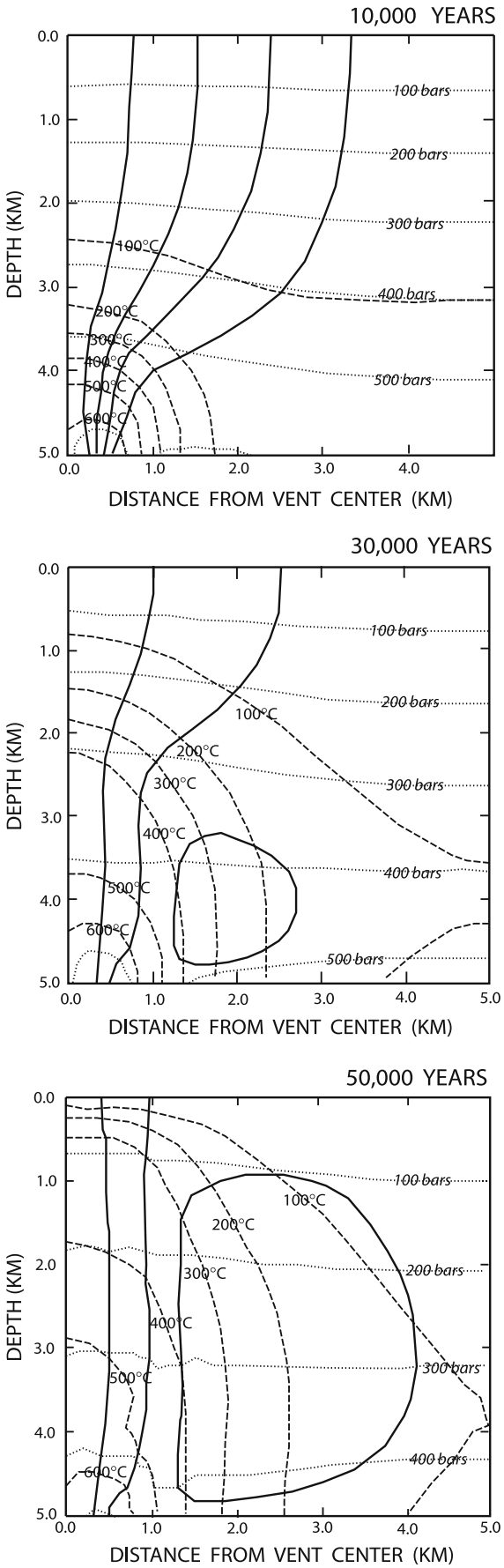

Fig. 7 Calculations showing the progressive focusing of hydrothermal venting when 700°C fluid is introduced at the left bottom boundary at 10 g cm^{-2} $year^{-1}$. Initially venting spreads in a horsetail to minimize flow resistance, but adjacent convection progressively focuses it into a plume across which total fluid pressure (*dotted lines*) is unchanged. If venting were more rapid and/or continued longer, discharge would approach the injection temperature of 700°C. From Cathles (1981)

The high-temperature 350°C venting is heated by magma, and magma (in the pore space of a cumulate or in a melt lens) must be present for it to occur. Fluids vent at ~350°C in all systems (intrusions on land or at ridges). How vent temperatures are so greatly reduced from the 1,200°C magma temperatures they could attain is a long-standing question. One possibility is that the thermodynamic properties of water will conspire to control venting in this range, and the advanced simulations carried out by Cormou that were reviewed in the section discussing convection above the melt lens shows that this is a viable possibility under certain conditions. Although this mechanism could well be operative above the melt lens, it is not clear that it is necessarily controlling for the convective system that operates at higher pressures below the melt lens where the convecting fluids have access to the near-vertical walls of the axial intrusions and the convection is forced rather than free.

The needed fully realistic fluid property simulations have not been carried out, but simulations I have carried out that include the heat transport impact of phase separation and the pressure-temperature dependence of fluid viscosity and density suggest that fluids which have access to the near-vertical margins of a magma intrusion will vent at close to the temperatures at which they are allowed to interact with the host and that the thermodynamic properties of water magnify this tendency (Cathles 1983). If correct, this means that seawater circulates through highly fractured (by thermal contraction; Lister 1976) rock adjacent to magma intrusions at ~350°C. Intensely veined greenschist zones observed in intrusions represent these flow zones (Schiffries and Skinner 1987; Ioannou and Spooner 2007). Based on this, I concluded that at temperatures greater than ~375 to 400°C fractures heal (by chemical dissolution and precipitation—a mineral reaction brittle–ductile transition) rapidly enough that little persistent flow through them is possible. The "350°C flow zone" is thus separated from pores containing melt by a zone through which there is no persistent flow and through which heat is transferred to the flow zone by conduction from 1,200°C magma.

This has some interesting implications. Under normal conditions of black smoker discharge, the width of the 350°C flow zone adjusts its width so that it carries off the conductively introduced heat and its internal pressure gradient is cold water hydrostatic and can keep the adjacent

cold waters at bay, as discussed above. If, in the highly active ridge axis environment, tectonic or magmatic disturbances caused the permeability of the flow zone to increase, its width will contract and a substantial portion of its 350°C fluid content could be expelled. For a brief period of time, the 350°C discharge across the seafloor can be greatly augmented (megaplume discharge). After the megaplume discharge, the venting will return to normal. For a while, the width of the 350°C flow zone will just be narrower (see Cathles 1993b).

Fracturing of the conduction zone adjacent to the 350°C flow zone is the likely explanation for the high-temperature veins that have very narrow or no vein halos and contain NaCl-rich amphiboles, inclusions with halite, and vein mineral assemblages suggesting temperatures of 600–800°C (Schiffries and Skinner 1987; Ioannou and Spooner 2007). Episodic thermal cracking of the thermal boundary layer (which sequesters salt and returns fresh water to the flow zone) followed by later migration of the 350°C flow zone into the now-salty thermal boundary zone (which is forced to eventually occur by seafloor spreading) can explain the observed salinity variations in black smoker and VMS ore fluids from about half to twice seawater levels as well as the changes in discharge rate of black smokers from normal to megaplume and back if the 350°C flow zone is ~3.4 m wide, 3.5×10^{-13} m^2 in permeability, separated from magma by ~180 m, and increases by 250-fold in permeability during a megaplume event (Cathles 1993b).

Baker et al. (1989) attribute megaplume discharge to extrusive flows. The distributed nature of extrusive flows makes it unlikely to me that they could produce large buoyancy plumes. Lowell and Xu (2000) examine whether an event plume could be produced by dike injection. They conclude that a dike would need a very permeable margin to produce an event plume and that a deeper magma heat source would be needed to support the 3 years of high-temperature venting that followed the megaplume events. Cann and Strens (1989) trapped hot fluids beneath a seal and then ruptured it to produce the megaplume, but a spreading ridge is not a good place to make a good seal and black smoker venting appears to have preceded and followed the megaplume events. On the other hand, the flow zone dynamic explanation is a natural and expected consequence of other observations (Elders Wairakei observations, Schifferies no-halo high-salinity veins, and salinity variations in the vent fluids). The natural mixing of different kinds of fluids it offers is a good potential explanation of the complex mixing relations between vapor, brine, and single phase fluids that is observed (Von Damm 1988, 2000).

The presence of black smokers means that magma is present in the pores of the gabbro cumulate near the ridge (or in a melt lens). Black smoker discharge occurs at intervals along the central part of the ridge axis that lies between transform faults where the elevation of the ridge is slightly higher (the shallowest or shoaling part of the ridge axis; Francheteau and Ballard 1983). The fraction of the ridge axis occupied by black smokers approximately equals the full spreading rate in millimeters per year times 0.004 year mm^{-1} (Baker et al. 1996). Thus, ~44% of a ridge spreading at 110 mm $year^{-1}$ (a fast-spreading ridge) is occupied by black smokers, whereas 12% of a slow-spreading ridge like the Mid-Atlantic Ridge (30 mm $year^{-1}$) is so occupied. The hydrothermal venting not only occupies a larger fraction of the ridge axis at fast-spreading ridges, but the venting zones also seem to be more continuous (less segmented). At the fastest-spreading ridges, the ridge elevation is occasionally the highest near transform faults. Hydrothermal venting and tube worms are present, and the ridge axis is the highest near the Clipperton transform on the East Pacific Rise, for example (Fornari and Embley 1995).

If we consider the present situation along mid-ocean ridges to be a snapshot in time and thus to reflect the probability, over time, of having magma present in the gabbro layer under and high-temperature vents along the ridge axis, we can conclude that spreading and high-temperature hydrothermal activity are nearly continuous in central locations between the transform offsets of fast- and superfast-spreading ridges but that seafloor spreading is episodic near the transforms and more generally along intermediate- and slow-spreading ridges. Where heat can be conducted (or convected by seawater convection) away more easily, for example near transform faults and along slow-spreading ridges where fault movement along the walls of the axial valley is greater, the magmas that invade the oceanic crust may be cooled sufficiently to act like superglue and stick the plate together so that it must be periodically re-broken. In such cases, spreading, magma invasion, and high-temperature venting occur episodically in time. Where the heat losses are less severe compared to the heat supplied by spreading (e.g., the central portions of fast-spreading ridges), the gabbro layer at the axis never freezes, the axis is not glued, and seafloor spreading and high-temperature venting are continuous. Small (1998) provides an interesting discussion of the episodicity of seafloor spreading. Episodicity is more extreme and more clearly seen in continental and island arc rifting, as discussed in the next section.

Episodic spreading could easily be a simple consequence of lithosphere elasticity. For example, based on calculations in Cathles and Hallam (1991), the accumulation of 0.4 kb of tensile stress in a plate 1,000 km wide (500 km either side of a ridge) could be released in ~300 years as the seafloor is extended at the axis by 230 m. A change in plate

stress of 0.4 kb is very low compared to what might be possible. The asthenosphere viscosity assumed in the 300-year time estimate is 10^{19} Pa s but could easily be much lower near the ridge axis, so the spreading pulse could last much less than 300 years. Periodic spreading near transform faults with steady spreading at the central parts of the ridge axis between transforms (like a butterfly flapping its wings) and general episodic spreading at slow-spreading ridges could thus be achieved by storing elastic energy in the oceanic lithosphere adjacent to glued portions of the spreading axis and retrieving it again when the axis ruptures.

The episodicity of seafloor spreading is important to our VMS discussion because episodic spreading could produce a non-uniform spatial distribution of seafloor mineralization. If hydrothermal venting at the axis is significantly delayed relative to the time required for the completion of the spreading event, sulfide material will be deposited in bands. Sulfides will be deposited after a strip of new crust is formed at the axial edge of the new strip. Mineralization along a ridge-perpendicular transect cutting across the central, between-transform portions of a fast-spreading ridge should be nearly continuous, but along a transect cutting the ridge near transform offsets, the metallization should form ridge-parallel bands that are separated from previous bands by barren crust, e.g., crust that has not had high-temperature hydrothermal fluids pass through it. At intermediate-spreading ridges, these bands should become more dominant relative to the continuous metallization and also become segmented as the hydrothermal activity along these ridges becomes segmented. At slow-spreading ridges, the mineralization may be entirely in discontinuous piles (see later discussion of TAG). Provided the accumulation efficiency of sulfides from black smoker vents is the same, the average metal mass per unit area of seafloor may be the same, but in some places, the mineralization may be swept into piles and in other places not. The size and separation of the piles should reflect the rate of spreading and the location of transform offsets of the ridge axis and perhaps also the size of the plate and the temperature of the asthenosphere near the ridge.

Finally, permeability is clearly controlled by fractures in the oceanic crust. The intimate fracturing produced by the drastic thermal quenching (from 1,200°C to 350°C) very near the ridge axis allows the intimate contact between the hydrothermal fluids and basalt that is needed to leach base metals from the basalt. Such leaching is observed (Richardson et al. 1987). Black smoker venting is almost always associated with minor faults (e.g., Fornari and Embley 1995). However, the spacing of black smokers can be very close at fast-spreading ridges or on magma mounds on slow-spreading ridges (<10 m at the TAG site near the Mid-Atlantic Ridge and at 9°49–50′ N on the East Pacific Rise, for example), yet can be much more widely spaced along other ridges or ridge segments (200–300 m in the axial graben at 13°N on the East Pacific Rise; Fornari and Embley 1995). Except perhaps at the very fastest-spreading segments, where the discharge is nearly continuous, the fracture spacing is much smaller than the vent spacing. Thus, the fractures seem to be opportunistically occupied near the locations where other factors dictate that the venting should occur.

Venting appears to occur with very little near-surface resistance at the ridge axis. The touchdown of the submersible that revisited the black smoker discovery site at 21° N restarted a black smoker, presumably by breaking a thin surface crust. This indicates that, at least at this site, there was not a great deal of surface resistance to venting that could drive long distance lateral flow along the axis. Venting seems to be unimpeded and of a single pass flow-through character, with little ponding of hydrothermal fluids in the subsurface. This is true for geothermal systems like Wairakei as well, where stratigraphic complexities could facilitate ponding but do not. The lack of significant resistance to venting very near the surface makes the generation of megaplumes from extrusive flows difficult. The concept of a geothermal "reservoir" may be a bit of a misnomer.

To summarize, the flux of metals carried to or across the seafloor is proportional to and measured by the thickness of the oceanic crust. It is greater where the mantle is hotter and the ocean crust thicker, greater in the thicker crust of a rifted island arc, and still greater where continental crust is rifted. The tonnage of VMS-type mineralization probably deposited on the ocean floor is huge compared to the resources of VMS mineralization so far discovered. Seafloor spreading (magma injection into ocean ridges) is often episodic and so, therefore, is the black smoker discharge that is tied to the presence of magma. Where the spreading is most episodic, the deposits should be the largest even though the metals accumulated is the same per unit area of ocean crust. Seawater convection clearly controls the shape and longevity of magma chambers (cumulates with magma in their pores). Fracturing and faulting of the oceanic crust controls its permeability but probably does not control the location of the black smoker hydrothermal vents, except very locally.

There are many other features of mid-ocean ridges that are of general interest. For example, small offsets of the ridge axis called devals occur between transform offsets, spreading centers can overlap, magmas can pond along ridges and collapse like mini-calderas, convection at the ridge axis and parallel to it may help control the spacing of black smoker discharge, etc. However, these are issues that we will just mention and now move to a discussion of the

features in the arc setting of VMS deposits that are different from those at mid-ocean ridges.

Island arc rifting, back-arc spreading, and VMS mineralization

Almost all VMS deposits mined were formed at arc or back-arc spreading centers. Franklin et al. (2005) assign all known VMS districts to the tectonic setting that produced them based on the district lithostratigraphy. They distinguish deposits formed during the initial rifting of an island arc (e.g., Abitibi, Matagami) and in progressively mature back-arc settings (Cyprus, Semail, and Besshi) and during the initial (Tasman and Hokuroku Districts) and more mature (Bathurst District and Iberian Pyrite Belt) rifting of continental arcs. Only a very few VMS districts formed in intracontinental rifts; Franklin et al. cite only the Laochang deposit in the PRC for this setting. VMS deposits that we mine today thus formed in arc and back-arc rifts, not on the ocean floor or in continental rifts.

The lack of VMS deposits in continental rifts may be a matter of classification. Continental rifts generally produce SEDEX deposits, a type of lead–zinc mineralization produced by basin brines. Modified seawater is the dominant ore fluid in the type of deposit we choose to call VMS (Franklin et al. 2005). Arcs have better access to seawater than intracontinental rifts and thus would tend to be dominated by seawater and form VMS deposits, whereas intracontinental rifts would tend to circulate brines and form SEDEX deposits. The same processes might be involved with the only difference being the salinity of the convecting fluid, which seems an insubstantial basis for defining a separate deposit type.

The reason that we lack examples of mined ocean floor massive sulfides is not that such deposits do not exist or are not rich enough to be mined. Many attractive deposits have been discovered on the seafloor (Hanington et al. 2005). Rather, it is that seafloor VMS-type deposits have a much lower probability of preservation in a subaerial setting where historically they would have been discovered and mined. Obduction of back-arc basin crust is quite likely when these basins close while subduction is the general fate of ocean crust in a closing ocean basin. To date, exploration and production has been solely for subaerial VMS deposits. We mine deposits formed in arc and back-arc crust that has been obducted.

Magmas in the arc and back-arc setting differ chemically from those at mid-ocean ridge setting because subduction carries water (and perhaps sediment and metal sulfides) into the mantle. Hydration produces the arc volcanism. When the arcs are rifted, magmas produced by mantle decompression are also produced. Their volume is greater than the arc magmas, but they mix with them and the magma chemistry is more complex because of this. As the center of back-arc spreading moves away from the arc, the magmas are increasingly dominated by decompression melts of the same mid-ocean ridge basalt composition that is found at mid-ocean ridges (Taylor and Martinez 2003) Magmatic aqueous fluids contribute to VMS deposits formed in the arc and near arc setting (Yang and Scott 2006), but the dominant cause of VMS mineralization even here is probably the intimate cracking of magmas and the extraction of metal by convecting pore fluids of modified seawater composition. Even if this is not so, we can distinguish the VMS-type as an end-member style of mineralization and simply allow that in some settings it will be mixed with other styles of mineralization, such as the porphyry style in which metals are provided by aqueous volatiles exsolved from magma rather than by the convective interaction of seawater with quenched magmas.

With this said, the main difference between VMS mineralization in arc and back-arc settings and at mid-ocean ridges is that the former are often associated with sill intrusions and the magmatism that produces the mineralization is a short-lived often singular event. The VMS deposits in a district typically lie on or very near a single age horizon, and the district is often underlain by a mafic sill. The situation is particularly clear in the Matagami district of Quebec where almost every discovered deposit lies on the key tuffite marker horizon situated about 2 km above the Bell River Complex sill. The thickness of this sill tapers from a central maximum of ~6 to 0 km over a distance of ~30 km (Carr et al. 2009). By the classification of Franklin et al. (2005), Matagami is a bimodal-felsic district that formed in the initial stages of arc rifting. The situation is slightly more complex at the Noranda VMS district in Quebec, which Franklin et al. also place in the bimodal-felsic category. Here, as in many VMS districts (Galley 2003), deposits formed above a composite sill (the Flavrian pluton) and are located at five time-stratigraphic horizons within five volcanic cycles. Most of the deposits and nearly all the ore tonnage are associated with the third volcanic cycle, however (Gibson and Watkinson 1990).

The VMS deposits in the Hokuroku district of Japan formed during the incipient (and in this case subsequently aborted) rifting of a several-times-previously-rifted continental margin, and all the deposits in this district lie along a common age horizon. The Hokuroku VMS district lies in a ~30-km-wide topographically low area between two chains of volcanoes that have been active in Quaternary time. The district was a basin that accumulated turbidites and coarse clastic rocks at the beginning of the Miocene. Beginning in the Miocene, the area subsided from subaerial to a sufficient water depth to prevent boiling (>1.5 km below sea level). VMS deposits formed on the seafloor at the

boundary of the Nishikurosawa and Onagawa formations in middle-Miocene time. The ore horizon subsequently rose to ~500 m below sea level (see papers in Ohmoto and Skinner 1983).

The history of rifting of the Japanese island arc and the cause for the subsidence and subsequent uplift of the Hokuroku District is illustrated in Fig. 8. The subsidence and ore deposits were formed when the island arc of Japan rifted. The subsidence was the result of a dynamic loss of hydraulic head of mantle material flowing into the opening rift. The cause is the same as that which produces the deep axial graben at slow-spreading mid-ocean ridges. The spreading episode was rapid because it was propelled by the elastic snapback of the Asian plate. Arc magmas subsequently re-glued the rift, and when spreading ceased, the dynamic loss of fluid head was recovered and the Hokuroku basin rose to its present elevation. The deposits were protected in the stable setting of the re-glued rift and invulnerable to erosion at their slightly sub-sealevel elevation. As shown in Fig. 8, the Japanese arc had rifted several times before, and presumably VMS deposits were produced each time. The last rifting failed (was aborted) and the VMS deposits were preserved in a position where they could easily be discovered and mined.

The rapid spreading produced by the elastic snapback appears to be a good way to emplace shallow sills. Presumably the melts produced by mantle decompression rise easily upward to their level of density stratification and then move outward. VMS deposits form as seawater convection cools the sill. Recent numerical models illustrate how this convection cools the sill from the bottom as well as the top and show that the spacing and size distribution of VMS deposits is a natural result of the sill geometry and the convective flow it induces, provided the zones of model hydrothermal upwelling are locked into place soon after they are initiated (by a temperature-dependent rock permeability). The locking of hydrothermal discharge pathways seems to occur in nature. The TAG black smoker field, located 2.4 km from the axis of the Mid-Atlantic Ridge, has been periodically active since it was at the ridge axis (Humphris and Tivey 2000). Simulations suggest that a single large deposit dominates the ore tonnage of a district more when the permeability of the host invaded by the sill is larger. The total tons of metal transported across the district seafloor is maximum for a sill depth of 2 km and a host permeability of 10^{-15} m^2. Deposits of the size discovered at Matagami are produced if the model accumulation efficiency is ~3% (Carr et al. 2009).

We thus see that exactly the same principles apply to VMS deposits formed in rifted arcs as in a mid-ocean ridge setting. The episodicity of the rifting is exaggerated, at least in the initial stages of arc rifting. In this setting, only one or at most a few spreading pulses produce all or most of the mineralization. Magma sills drive the seawater convection rather than more tabular magma intrusions in the gabbro layer of the ocean crust. In more mature back-arc rifts such as perhaps (it could be ocean ridge) the Samail Ophiolite in Oman, intrusions may be more tabular and similar to those at mid-ocean rifts. Single-pass flow-through convection of the type discussed in the mid-ocean ridge section replicates the oxygen isotopic alteration observed there (Cathles 1983). The district-wide surface metal surface density is proportional to the thickness of the magma intrusion. Whether it is of sill geometry or of the geometry of the gabbro layer of the ocean crust is of no consequence.

One final matter of great significance remains. From Fig. 5, it is clear that, assuming a substantial fraction of the crust invaded by magma in VMS districts, the efficiency of metal accumulation becomes the most important resource factor. If the efficiency of accumulation were 30% rather than 3%, or 0.3% rather than 3%, the resources in a district

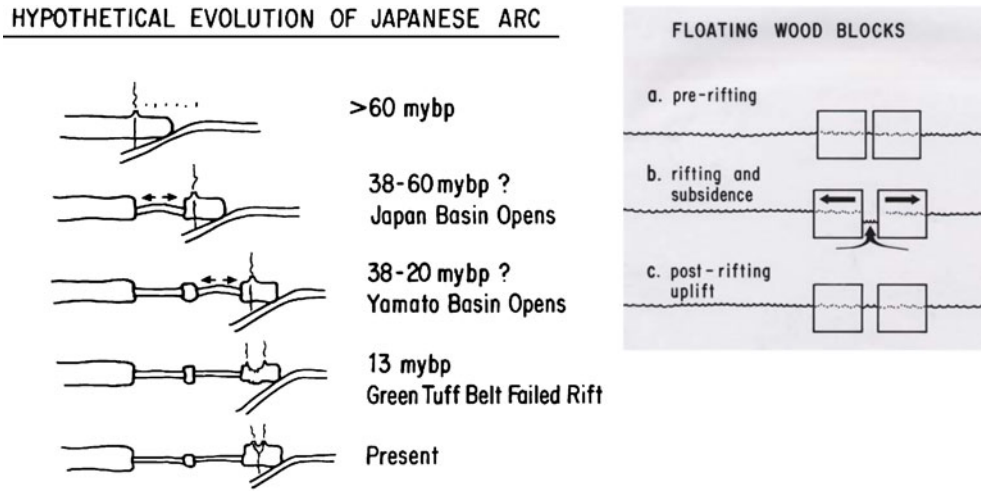

Fig. 8 The Hokuroku VMS district was formed in middle-Miocene time when the island arc of Japan rifted. The area subsided due to a hydraulic loss of fluid head as asthenospheric material sought to fill the rift, as illustrated by the floating wood blocks to the left. The area uplifted when the rifting aborted. Figures from Cathles et al. (1983)

would be comparatively spectacular or very lean. Of the factors that affect metal accumulation efficiency, the most important by far appears to be the facility with which metal is trapped below the surface, or more precisely before the hot fluids enter and mix with ocean water. The trapping efficiency at the seafloor increases with time as biota are able to construct chimneys that are effective in cooling the vent fluids and precipitating their metal content before they are discharged into the ocean. Thus, vents that are able to operate for long periods of time undisturbed by lava flows or factors that would kill vent biota are likely to produce larger sulfide accumulations. Sulfide mounds appear to have very high internal permeability which allows them to locally distribute high-temperature fluids and vent them in a diffuse fashion. For example, Schultz et al. (1992) measure the diffuse venting from a 25-m^2 sulfide mound on the ridge crest of the Endeavor segment of the Juan de Fuca Ridge and show that ~2.9 MW is vented by its single black smoker whereas 58 MW is vented diffusely at low temperatures across the tubeworm-covered mound. The distribution of flow occurring in this mound increases the metal accumulation efficiency ~20-fold. The chemical evolution and zone refinement of sulfide mounds is described by Eldridge et al. (1983). Fluid dynamics and permeability in sulfide mounds is discussed in Cathles (1983). The result of extreme zone refinement is barren siliceous pyrite. The overall message is that diffuse leakage can greatly increase metal accumulation efficiency and also change the metal mix, increasing the copper grade at the expense of Zn and Fe (as long as the throughput is not too excessive).

Metal trapping in sulfide mounds and by sulfides in the feeder pipes of VMS deposits by cooling-induced open space filling or replacement of sulfide material is important, but the open space filling and replacement in silicates may be an even more important mechanism for increasing district and deposit resources. Silicate replacement is indicated where sulfide lenses are enclosed in rapidly accumulating pumice or volcanoclastic debris or turbidite flows, especially if there are relics of the original silicates, reaction fronts separating sulfide and silicate, or if the sulfides cross-cut the stratigraphy (Galley et al. 1995; Doyle and Huston 1999; Doyle and Allen 2003; Franklin et al. 2005). Sulfide replacement of silicates occurs very near the surface and is most common in pumice ash deposits and the quenched margins of lavas and intrusions. A sedimentary architecture that encourages the near-surface dispersal of hydrothermal upflow, such as laterally extensive permeable turbidite or sand layers, promotes replacement. Some of the largest VMS deposits are thought to be of replacement type. An example is the Horn H deposit in which the sulfides are also strongly zone refined, suggesting continued hydrothermal throughput.

Summary and discussion

In the preceding paragraphs, we have looked broadly at the style of hydrothermal convection that is associated with seafloor spreading, perhaps the single most widespread and important process affecting our planet. From the pattern of measured heat flow and other observations, it is clear that all the heat introduced to the oceanic crust by seafloor spreading is carried out of the crust at the spreading axes by 350°C aqueous fluids of modified seawater composition. The mass of 350°C fluid circulated across each unit area of seafloor (or so close to the seafloor that its heat content is conductively discharged to the ocean) equals the mass per unit area of magma intrusion (the gabbro layer thickness). If 100% of the base metals carried to or across the seafloor by this circulation accumulated on the seafloor, the seafloor would be a giant VMS district 30 to 100 times more richly endowed with base metals per unit surface area than the VMS districts we presently mine. If the base metal accumulation efficiency on the ocean crust is similar to the 3% observed at 21° N on the East Pacific Rise and in VMS districts, the ocean floor metal content per unit area would be similar to that in currently mined VMS districts but the total ocean metal resources would be over 600 times greater than the present (land) VMS metal resources. Seafloor spreading at slow-spreading mid-ocean ridges and near transform faults at fast-spreading ridges is episodic and so therefore is the formation of axial magma intrusions and high-temperature, sulfide-depositing hydrothermal circulation. Arcs rift more episodically than mid-ocean ridges and, at least for VMS deposits formed in the initial stages of arc rifting, hydrothermal circulation is driven by sills rather than the more tabular magma intrusions that drive hydrothermal circulation at mid-ocean ridges. However, the basic principles remain the same. One kilogram of magma intrusion drives 1 kg of 350°C hydrothermal circulation, and the potential average district metal endowment is proportional to sill thickness. Sill-driven circulation predicts a deposit tonnage distribution (Snow White and the Seven Dwarfs) and spacing similar to that observed in districts like Matagami. Given substantial invasion of a district by magma, the main determinant of district endowment is the efficiency with which metals are accumulated near the seafloor. This accumulation efficiency can be increased greatly by a near-surface stratigraphy that diffuses upwelling convection and allows near-subsurface cooling of the 350°C fluids because, under these conditions, not only can sulfides be precipitated into open pore spaces but silicate minerals also can be replaced by sulfides. The very large VMS deposits in the Iberian Pyrite Belt may be a consequence of the thick crust and complex near-surface stratigraphy present there.

This is a simple story that rests mainly on observations interpreted through a few guiding principles. Exploration implications are as follows: (1) Arcs will be rift prone or

not depending upon the relative motion of the over-riding plate. If its absolute motion is away from the trench, as is Asia today, the arc will be rift prone and a good place to seek VMS mineralization. (2) There will be a very brief time interval during the rifting of an arc at which VMS deposits will form in districts all along the arc. Finding the ore horizon in one district will guide exploration to the right time-stratigraphic interval in other districts (transform offset segments) of the arc. If the spreading pulse opens like a zipper, the times may not be identical but should be in a regular progression. (3) Because of the dynamic loss of asthenosphere head, districts should be local depressions at the time of ore deposition; basins that receive turbiditic flows at the time of mineralization like the Hokuroku Basin in mid-Miocene Japan or the Guaymas Basin in the Gulf of California today. (4) Excessive zone refinement by too much hydrothermal flow through a sulfide mounds may remove all base metals leaving only pyrite. In this case, areas of weaker or shorter duration discharge should be sought. (5) All fluids (magmas as well as hydrothermal aqueous fluids) will utilize the permeable fractures that may locally control the position of VMS mineralization. The feeder zones of basalt flows and rhyolite domes will be equally prospective locations. (6) Alteration patterns, especially a depletion of ^{18}O around intrusions, can reveal whether the intrusions have driven the kind of hydrothermal convection that could produce VMS deposits (Cathles 1993a). (7) The spacing and relative size of deposits is controlled by the depth of burial and geometry of the sill that drives hydrothermal convection. Fractures and faults generally will be opportunistically utilized and affect the location of discharge and VMS mineralization only slightly. (8) There are many processes that can complicate convection above a melt lens or sill, but fluid properties and the tendency for venting to operate at the greatest efficiency possible (highest Nusselt number) and simple factors like the slope of the intrusion top may also simplify the pattern of convection enough to provide useful exploration insights.

We should know more about how episodic spreading at ridges occurs (the flapping of butterfly wings). We should know more about how hydrothermal circulation locks itself into position. The enhanced permeability of the 350°C flow zone and how this zone moves with time through the conductive boundary layer toward magma needs more study. Whether it is a consequence of dynamic rock permeability (thermal cracking and temperature controlled healing) or fluid properties will be interesting to determine. It seems unlikely that ridge-parallel or ridge-perpendicular convection could ignore completely both the 350–400 and the ~700°C brittle–ductile transitions. A clearer demonstration that fluid properties cannot restrict venting temperature if fluids access the near-vertical margins of an intrusion would be useful. The reasons for high salinities in some VMS systems such as the Matagami (16.2±4.7 wt.%) and the low-temperature operation of these systems (208±32°C), which may be related to the ponding of brine on the top of a sill (Ioannou et al. 2007), need further investigation. It would be interesting to know more about how sills form in rifting arcs and what determines (or even what was) their geometry at the time of VMS formation.

The broad process view of this paper suggests that we are currently utilizing only the most accessible VMS-type deposits. The ocean floor is, comparatively, an almost unimaginably large resource from which we may someday extract metals. VMS ore deposits are the consequences of and provide information on the most fundamental earth processes. In seeking to explore more effectively for them, we also pose scientific questions regarding the operation of important earth processes. Exploration generates the detailed data that can help answer these questions, and insights from observation and modeling of the mid-ocean hydrothermal systems are of huge value. More effective exchange of insights between interest groups (geothermal, ocean ridge, ore deposit, modeling) and over time (early and later studies) could facilitate progress.

Acknowledgments The idea that VMS deposition could be quantitatively related to the crustal heat removed by convection at mid-ocean ridges occurred to me in 1982 when Steve Scott, Mike Mottl, Kirt Shusterich, and I spent a fabulously stimulating summer working in Bob Ballard's barn to produce a report to industry on the connection between the then recently discovered ocean hydrothermal vents and massive sulfide mineralization. Mid-ocean ridge processes have been a fascination of mine ever since. Fernando Tornos encouraged me to contribute a broad perspective paper to this volume, and an anonymous reviewer suggested material that could be added. I am indebted to and thank these colleagues for their contributions.

References

Baker ET, Lavelle JW, Feely A, Massoth GJ, Walker SL (1989) Episodic venting of hydrothermal fluids from the Juan de Fuca Ridge. J Geophys Res 94(B7):9237–9250

Baker ET, Chen YJ, Phipps Morgan J (1996) The relationship between near-axis hydrothermal cooling and the spreading rate at mid-ocean ridges. Earth Planet Sci Lett 142:137–145

Bishoff JL, Rosenbauer RL (1985) An empirical equation of state for hydrothermal seawater (3.2 percent NaCl). Am J Sci 285:725–763

Cann JR, Strens MR (1989) Modeling periodic megaplume emission by black smoker systems. J Geophys Res 94:12,227–12,237

Carr P, Cathles LM, Barrie CT (2009) On the size and spacing of VMS deposits within a district, with application to the Matagami District, Quebec. Econ Geol 103:1395–1409

Cathles LM (1977) An analysis of the cooling of intrusives by ground water convection which includes boiling. Econ Geol 72:804–826

Cathles LM (1978) Hydrodynamic constraints on the formation of Kuroko deposits. Mining Geology 28:257–265

Cathles LM (1981) Fluid flow and hydrothermal ore deposits. Economic Geology 75th Anniversary Volume:424–457

Cathles LM (1983) An analysis of the hydrothermal system responsible for massive sulfide deposition in the Hokuroku Basin of Japan. Econ Geol Monogr 5:439–487

Cathles LM (1993a) Oxygen isotope alteration in the Noranda Mining District, Abitibi greenstone belt, Quebec, Canada. Econ Geol 88 (6):1483–1512

Cathles LM (1993b) A capless 350° flow zone model to explain megaplumes, salinity variations, and high-temperature veins in ridge axis hydrothermal systems. Econ Geol 88(8):1977–1988

Cathles LM (1997) Thermal aspects of ore formation. In: Barnes HL (ed) Geochemistry of hydrothermal ore deposits. Wiley, New York, pp 191–227

Cathles LM, Hallam A (1991) Stress induced changes in plate density, vail sequences, epeirogeny, and short-lived global sea level fluctuations. Tectonics 10:659–671

Cathles LM, Guber AL, Lenagh TC and Dudas FO (1983) Kuroko type massive sulfide deposits: products of an aborted island arc rift. Econ Geol Monogr 5:96–114.

Chen YJ (2000) Dependence of crustal accretion and ridge-axis topography on spreading rate, mantle temperature, and hydrothermal cooling. Geol Soc Am Spec Pap 349:161–179

Cherkaui ASM, Wilcock WSD, Dunn RA, Toomey DG (2003) A numerical model of hydrothermal cooling and crustal accretion at a fast-spreading mid-ocean ridge. Geochemistry Geophysics and Geosystems 4(9):8616. doi:10.1029/2001GC000215

Cochran JR, Buck WR (2001) Near-axis subsidence rates, hydrothermal circulation, and thermal structure of min-ocean ridge crests. J Geophys Res 106(B9):19233–19258

Converse DR, Holland HD, Edmond JM (1984) Flow rates in the axial hot springs of the East Pacific Rise (21N): implications for the heat budget and the formation of massive sulfice deposits. Earth Planet Sci Lett 69:159–175

Cormou D, Driesner T, Heinrich CA (2006) The dynamics of mid-ocean ridge hydrothermal systems: splitting plumes and fluctuating vent temperatures. Earth Planet Sci Lett 245:218–231

Cormou D, Driesner T, Heinrich CA (2008a) Heat transport at boiling, near-critical conditions. Geofluids 8:208–215

Cormou D, Driesner T, Heinrich CA (2008b) The structure and dynamics of mid-ocean ridge hydrothermal systems. Science 321:1825–1828

Davis EE, Chapman DS, Wang K, Fisher AT, Robinson SW, Gringel J, Pribnow D, Becker K (1999) Regional heat flow variations across the sedimented Juan de Fuca Ridge eastern flank: constraints on lithospheric cooling and lateral heat transport. J Geophys Res 104(B8):17675–17688

Doyle MG, Allen RL (2003) Subsea-floor replacement in volcanic-hosted massive sulfide deposits. Ore Geol Rev 23:183–222

Doyle MG, Huston DL (1999) The subsea-floor replacement origin of the Ordovician Highway-Reward volcanic-associated massive sulfide deposit, Mount Windsor Subprovince, Australia. Econ Geol 94:825–844

Dunn RA, Forsyth DW (2003) Imaging the transition between the region of mantle melt generation and the crustal magma chamber beneath the East Pacific Rise with short-period Love waves. J Geophys Res 108(B7):2352. doi:0.1029/2002JB002217

Dunn RA, Toomey DR, Solomon SC (2000) Three-dimensional seismic structure and physical properties of the crust and shallow mantle beneath the East Pacific Rise at 9°30′N. J Geophys Res 105(B10):23537–23555

Elder JW (1966) Heat and mass transfer in the earth: hydrothermal systems. New Zealand Department of Scientific and Industrial Research Bulletin 169:1–115

Elderfield H, Schultz A (1996) Mid-ocean ridge hydrothermal fluxes and the chemical composition of the ocean. Annu Rev Earth Planet Sci 24:191–224

Eldridge CS, Barton PB, Ohmoto H (1983) Mineral textures and their bearing on formation of Kuroko orebodies. Econ Geol Monogr 5:241–281

Emmanuel S, Berkowitz B (2007) Phase separation and convection in heterogeneous porous media: implications for seafloor hydrothermal systems. J Geophys Res 112:B05210

Fehn U, Green KE, Von Herzen RP, Cathles LM (1983) Numerical models for the hydrothermal field at the Galapagos spreading center. J Geophys Res 88(B2):1033–1048

Fontaine FJ, Wilcock WSD (2006) Dynamics and storage of brine at mid-ocean ridge hydrothermal systems. J Geophys Res 111: B06102. doi:10.1029/2005JB003866

Fontaine FJ, Wilcock WSD (2007) Two-dimensional numerical models of open-top hydrothermal convection at high Raleigh and Nusselt numbers: implications for mid-ocean ridge hydrothermal circulation. Geochemistry Geophysics Geosystems 8(7): Q07010. doi:10.1029/2007GC001601

Fontaine FJ, Rabinowicz M, Boulegue J (2001) Permeability changes due to mineral diagenesis in fractured crust: implications for hydrothermal circulation at mid-ocean ridge. Earth Planet Sci Lett 184:407–425

Fontaine FJ, Wilock WSD, Butterfield DA (2007) Physical controls on the salinity of mid-ocean ridge hydrothermal vent fluids. Earth Planet Sci Lett 257:132–145

Fontaine FJ, Cannat M, Escartin J (2009) Hydrothermal circulation at slow-spreading mid-ocean ridges: the role of along-axis variations in axial lithospheric thickness. Geology 36:759–762

Fornari DJ, Embley RW (1995) Tectonic and volcanic controls on hydrothermal processes at the mid-ocean ridge: an overview based on near-bottom and submersible studies. In: Humphris SE, Zierenberg RA, Mullineaux LS, Thomson RE (eds) Seafloor hydrothermal systems: physical, chemical, biological, and geological interactions. Geophysical monograph 91. American Geophysical Union, Washington, D.C., pp 1–46

Francheteau J, Ballard RD (1983) The East Pacific Rise near 21°N, 13°N and 20°S: inferences for along-strike variability of axial processes of the mid-ocean ridge. Earth Planet Sci Lett 64:93–116

Franklin JM, Gibson HL, Jonasson IR, Galley AG (2005) Volcanogenic massive sulfide deposits. Society of Economic Geology 100th Anniversary Volume:523–560

Galley AG (2003) Composite synvolcanic intrusions associated with Precambrian VMS-related hydrothermal systems. Miner Deposita 38:443–473

Galley AG, Watkinson DH, Johasson IR, Riverin G (1995) The subea-floor formation of volcanic-hosted sulfide: evidence from the Ansil deposit, Rouyn-Noranda, Canada. Econ Geol 90:2006–2017

Gibson HL, Watkinson DH (1990) Volcanogenic massive sulfide deposits of the Noranda Cauldron and shield volcano, Quebec. CIM Spec Vol 43:119–132

Gibson HL, Watkinson DH, Comba CDA (1989) Subaqueous phreatomagmatic explosion breccias at Buttercup Hill, Noranda, Quebec. Can J Earth Sci 26(7):1428–1439

Hanington MD, de Ronde CEJ, Petersen S (2005) Sea-floor and submarine hydrothermal systems. Society of Economic Geology 100th Anniversary Volume:111–141

Hirth G, Escartin J, Lin J (1998) The rheology of the lower oceanic crust: implications for lithospheric deformation at mid-ocean ridges. In: Buck WR et al (eds) Faulting and magmatism at mid-ocean ridges. Geophysical monograph series 106. American Geophysical Union, Washington, D.C., pp 291–303

Humphris SE, Tivey MK (2000) A synthesis of geological and geochemical investigation of the TAG hydrothermal field: insights into fluid-flow and mixing processes. Geol Soc Am Spec Pap 349:213–235

Ioannou SE, Spooner ETC (2007) Fracture analysis of a volcanogenic massive sulfide-related hydrothermal cracking zone, Upper Bell

River Complex, Matagami, Quebec: application of permeability tensor theory. Econ Geol 104(4):667–690

Ioannou SE, Spooner ETC, Barrie CT (2007) Fluid temperature and salinity characteristics of the Matagami volcanogenic massive sulfide district, Quebec. Econ Geol 104(4):691–716

Jupp T, Schultz A (2000) A thermodynamic explanation for black smoker temperatures. Nature 403:880–883

Lister CRB (1976) On the penetration of water into hot rock. Journal of the Royal Astronomical Society 39:465–509

Lowell RP, Burnell DK (1991) Mathematical modeling of conductive heat transfer from a freezing, convecting magma chamber to a single pass hydrothermal system: implications for seafloor black smokers. Earth Planet Sci Lett 104:59–69

Lowell RP, Germanovich LN (1994) On the temporal evolution of high-temperature hydrothermal systems ad ocean ridge crests. J Geophys Res 99(B1):565–575

Lowell RP, Xu W (2000) Sub-critical two-phase seawater convection near a dike. Earth Planet Sci Lett 174:385–396

Mottl MJ (2003) Partitioning of energy and mass fluxes between mid-ocean ridge axes and flanks at high and low temperature. In: Halbach PE, Tunnicliffe V, Hein JR (eds) Energy and mass transfer in marine hydrothermal systems. Dahlem University Press, Berlin, pp 271–286

Norton D, Cathles LM (1979) Thermal aspects of ore deposition. In: Barnes HL (ed) Geochemistry of hydrothermal ore deposits. Wiley, New York, pp 611–631

Ohmoto H, Skinner BJ (eds) (1983) Kuroko and related volcanogenic massive sulfide deposits. Econ Geol Monogr 5, pp 604 p

Pan Y, Batiza R (2003) Magmatic processes under mid-ocean ridges: a detailed mineralogic study of lavas from the East Pacific Rise 9° 30′N, 10°30′N, and 11°20′N. Geochemistry Geophysics Geosystems 4(11):8623. doi:10.1029/2002GC000309

Parsons B (1981) The rate of plate creation and consumption. Geophys J. R. Astro. Soc. 67:437–448.

Phipps Morgan J, Chen YJ (1993) The genesis of oceanic crust: magma injection, hydrothermal circulation, and crustal flow. J Geophys Res 98(B4):6283–6297

Ribando RJ, Torrance KE, Turcotte DL (1976) Numerical models for hydrothermal circulation in the oceanic crust. J Geophys Res 81:3007–3012

Richardson CJ, Cann JR, Richards H, Cowan JG (1987) Metal-depleted roots of the Troodos ore-forming hydrothermal systems, Cyprus. Earth Planet Sci Lett 84:243–353

Ridley IW, Perfit MR, Smith MC, Fornari DJ (2006) Magmatic processes in developing oceanic crust revealed in a cumulate xenolith collected at the East Pacific Rise, 9°50′N. Geochemistry Geophysics Geosystems 7(12):Q12O04. doi:10.1029/2006GC001316

Rosenberg ND, Fisher AT, Stein JS (2000) Large-scale lateral heat and fluid transport in the seafloor: revisiting the well-mixed aquifer model. Earth Planet Sci Lett 182:93–101

Sangster DF (1980) Quantitative characteristics of volcanogenic massive sulfide deposits: 1. Metal content and size distribution of massive sulfide deposits and volcanic centers. Canadian Institute of Mining Bulletin 73:74–81

Schiffries CM, Skinner BJ (1987) The Bushveld hydrothermal system: field and petrologic evidence. Am J Sci 260:115–141

Schoofs S, Spera FJ, Hansen U (1999) Chaotic thermohaline convection in low-porosity hydrothermal systems. Earth Planet Sci Lett 174:213–229

Schultz A, Delaney JR, McDuff RE (1992) On the partitioning of heat flux between diffuse and point source seafloor venting. J Geophys Res 97(B9):12,299–12,314

Small C (1998) Global systematics of mid-ocean ridge morphology. In: Buck WR, Delaney PT, Karson JA, Lagabrielle Y (eds) Faulting and magmatism at mid-ocean ridges. Geophys Monogr 106. American Geophysical Union, Washington, D.C., pp 1–25

Stein CA, Stein S (1994) Constraints on hydrothermal fluid flux through the oceanic lithosphere from global heat flow. J Geophys Res 99(B2):3081–3095

Solomon M (1980) Hot-water plumes on the ocean floor: clues to submarine ore formation. J Geol Soc Aust 27:89–90

Taylor B, Martinez F (2003) Back-arc basin basalt systematics. Earth Planet Sci Lett 210:481–497

Von Damm KL (1988) Systematics of and postulated controls on submarine hydrothermal solution chemistry. J Geophys Res 93 (B5):4551–4561

Von Damm KL (2000) Chemistry of hydrothermal vent fluids from 9-10N, East Pacific Rise: “time zero”, the immediate posteruptive period. J Geophys Res 105(B5):11203–11222

Von Damm KL, Buttermore LG et al (1997) Direct observation of the evolution of a seafloor ‘black smoker’ from vapor to brine. Earth Planet Sci Lett 149:101–111

Wilcock WSD (1998) Cellular convection models of mid-ocean ridge hydrothermal circulation and the temperatures of black smoker fluids. J Geophys Res 103(B2):2585–2596

Wolery TJ, Sleep NH (1976) Hydrothermal circulation and geochemical flux at mid-ocean ridges. J Geol 84(3):249–275

Yang K, Scott SD (2006) Magmatic fluids as a source of metals in seafloor hydrothermal systems. In: Christie DM, Fisher CR, Lee S-M, Givens S (eds) Back-arc spreading systems: geological, biological, chemical, and physical interactions. Geophysical monograph series 166. American Geophysical Union, Washington, D.C., pp 163–184